Journal of Marine Research, 48, 37–53, 1990

Barotropic variability in the presence of an ocean gyre

by Richard J. Greatbatch[1] and Jin Li[1]

ABSTRACT

We describe results from some idealized numerical calculations in which we examine the influence of a barotropically stable mean flow on wind-driven variability in a flat-bottomed barotropic vorticity equation model. The mean flow has features in common with the vertically integrated time-mean circulation found in eddy-resolving models with a Sverdrup interior, western boundary current and inertial recirculation region. We integrate the equations of motion linearized about this flow and driven by oscillating wind forcing and compare the results with those obtained when the mean state is one of rest. We find that the presence of a mean flow leads to significant distortion of the model response particularly near the western boundary and in the inertial recirculation region. This distortion is characterized by downstream amplification and phase lag compared to the rest mean state cases. It is related, on the one hand, to the distortion of the mean potential vorticity contours from lines of latitude and, on the other, to advection by the mean flow. Possible applications of these results are discussed to explain features of observed variability in the Gulf Stream system and also the anomalous southward intrusion of the Oyashio Current along the coast of Japan.

1. Introduction

It is well known that in the interior of the midlatitude ocean, the vertically integrated transport and the nonisostatic component of sea level are likely to vary in essentially the same way as in an ocean of uniform density for time scales of the annual period and less (Gill and Niiler, 1973; Anderson *et al.,* 1979; Anderson and Corry, 1985a). Even near coastal boundaries, where a baroclinic Kelvin wave can interact with topography, thereby driving vertically integrated transport by means of the JEBAR effect (Huthnance, 1984; Anderson and Corry, 1985a) a uniform density model can still provide useful information. For example, in their study of the seasonal variation of transport through the Florida Straits, Anderson and Corry (1985b) showed that a uniform density model captured a large part (in particular the phase) of the response seen in a two-density layer model. Also, Greatbatch and Goulding (1989a, b) have shown that a uniform density model can often capture the phase of the seasonal variation of adjusted sea level at coastal stations although the amplitude is usually underestimated. The

1. Department of Physics and Ocean Science Centre, Memorial University of Newfoundland, St. John's Newfoundland, Canada, A1B 3X7.

model of Greatbatch and Goulding (1989a) was particularly successful along the southeastern seaboard of the United States where they showed that the coastal sea level in the model is largely determined by the model predicted transport variations offshore. This lends support to Blaha's (1984) conclusion that coastal sea level in the region is strongly influenced by transport variations in the Gulf Stream and, indeed, it is well known (Maul *et al.*, 1985) that at the annual period or less, sea level fluctuations at Miami are a good indicator of transport variations in the Florida Straits. However, Greatbatch and Goulding's model could not adequately reproduce the summer minimum in sea level at Norfolk, Virginia, despite the fact that this feature is reproduced farther south. One possible explanation for this is that advection by the mean flow of the Gulf Stream, not accounted for in the model, is responsible for carrying the signal northward to Norfolk. Taking 1 ms^{-1} to be a representative velocity for the Gulf Stream in the area, the advection time from Miami to Norfolk is between two and three weeks. This is within the monthly mean time scale of the sea level data and suggests that the advection mechanism deserves further investigation.

It is also possible that the absence of a mean flow in the models of Anderson and Corry (1985b) and Greatbatch and Goulding (1989a) could explain the failure of these models to properly account for the amplitude of the observed seasonal variation of transport through the Florida Straits. Both models underestimate this signal by roughly a factor of 2. It has been noted (Schott and Zantopp, 1985) that the monthly mean surface wind stress curl over the western Caribbean has a seasonal variation very similar to that of transport through the Straits. It is possible that the mean flow of the Loop Current/Florida Current System is responsible for communicating the influence of these wind stress variations northward to the Straits.

In this paper, we describe results from the simplest possible model which can be used to investigate the influence of a mean flow—namely, a flat-bottomed barotropic vorticity equation model. We follow Böning (1986) by first spinning up a steady wind-driven gyre with features corresponding to those found in the "time-mean" in eddy-resolving general circulation models (e.g. Holland *et al.*, 1983). We then linearize the equations of motion about this state and examine variability in this system driven by an oscillating wind stress field and compare the results with those found when the equations are linearized about a state of rest. As we shall see, distortion of the potential vorticity field by the relative vorticity associated with the mean flow plays an important role in the model response in addition to advection by the mean flow.

Apart from the possible application of this work to the Gulf Stream system noted above, another application could be to understanding the anomalous southward intrusion of the Oyashio Current along the coast of Japan which takes place in some years in the spring. Sekine (1988a, b) has shown that this intrusion occurs in years when there is a positive wind stress curl anomaly over the North Pacific between about 30N and 45N in the previous winter (see Fig. 5 in Sekine, 1988a). He points out (Sekine, 1988b) that the lag between the appearance of the wind stress curl anomaly

and the occurrence of the intrusion, being no more than three months, is too short to permit an explanation in terms of baroclinic Rossby waves. A linear barotropic response, on the other hand, will take place on a time scale less than one month (Greatbatch and Goulding, 1989b) suggesting that perhaps advection by the mean flow association with the Oyashio also needs to be taken into account.

The plan of the remainder of this paper is as follows. Section 2 describes the model and the choice of the background mean state, corresponding to a time-averaged ocean gyre. In section 3 we present the results. Section 4 provides a summary and discussion in which we address, in particular, the limitations of our model and the relevance of our results.

2. The model

We consider a closed, square ocean basin of side πL and uniform depth H on a midlatitude β-plane. Using Cartesian coordinate axes, with x increasing eastward and y northward, the model is governed by the barotropic vorticity equation

$$\frac{\partial}{\partial t}(\nabla^2\psi) + J(\psi, \nabla^2\psi) + \beta\psi_x = \hat{\mathbf{k}} \cdot \frac{\nabla \times \tau}{\rho_o H} + K\nabla^4\psi \tag{1}$$

where ψ is the barotropic streamfunction ($u = -\psi_y$, $v = \psi_x$), t is time, $\hat{\mathbf{k}}$ is a unit vector in the vertical upward direction, τ is the surface wind stress, ρ_o a representative density for seawater and K a (uniform) horizontal eddy viscosity coefficient. J is the Jacobian operator

$$J(a, b) = -\frac{\partial a}{\partial y}\frac{\partial b}{\partial x} + \frac{\partial a}{\partial x}\frac{\partial b}{\partial y}.$$

Following Böning (1986) we write (1) in nondimensional form as

$$\frac{\partial}{\partial t^*}(\nabla^2\psi^*) + RJ(\psi^*, \nabla^2\psi^*) + \psi^*_{x^*} = F^* + E_L\nabla^4\psi^* \tag{2}$$

where R is the Rossby number, E_L is the (lateral) Ekman number and the following scaling has been used

$$(x, y) = L(x^*, y^*); \qquad t = t^*/\beta L; \qquad F = \left(\frac{\tau_o}{\rho_o HL}\right)F^*; \qquad \psi = \left(\frac{\tau_o}{\beta\rho_o H}\right)\psi^*. \tag{3}$$

In (2), $R = \tau_0/\rho_0 H\beta^2 L^3$ and $E_L = K/\beta L^3$. In (3), τ_0 is a scale for the magnitude of the surface wind stress and F denotes the wind stress curl forcing. We can also write (2) in the form

$$\frac{1}{R}\frac{\partial}{\partial t}q + J(\psi, q) = F + A\nabla^2 q \tag{4}$$

where now *'s have been dropped, $q = R\nabla^2\psi + y$ is the (nondimensional) potential vorticity and $A = E_L/R$.

Böning (1986) integrated (2) with steady wind forcing $\overline{F}$ for a square ocean basin like that considered here. His work differs from that of Bryan (1963) in the use of free slip boundary conditions.

$$\psi = 0, \qquad \nabla^2\psi = 0 \text{ along the boundary} \tag{5}$$

as distinct from no-slip. In this way, shear-flow instabilities in the western boundary layer are avoided and steady state solutions are found over a range of values of the Rossby number R, extending from the linear regime, where the solution is similar to that described by Munk (1950), to the highly nonlinear regime described by Briggs (1980). These solutions satisfy

$$J(\overline{\psi}, \overline{q}) = \overline{F} + A\nabla^2\overline{q} \tag{6}$$

or, equivalently,

$$RJ(\overline{\psi}, \nabla^2\overline{\psi}) + \overline{\psi}_x = \overline{F} + E_L\nabla^4\overline{\psi} \tag{7}$$

with $\overline{\psi} = \nabla^2\overline{\psi} = 0$ along the boundary. They are clearly completely determined by the values of R and E_L.

In this paper, we are concerned with the effect of perturbing one of Böning's steady state solutions by means of an oscillating wind stress curl F'. We therefore put $\psi = \overline{\psi} + \psi'$, and $q = \overline{q} + q'$ where $\overline{q} = R\nabla^2\overline{\psi} + y$, $q' = R\nabla^2\psi'$ and prime denotes perturbation from the mean state. Substituting into (4) and using (6) gives

$$\frac{1}{R}\frac{\partial q'}{\partial t} + J(\overline{\psi}, q') + J(\psi', \overline{q}) + J(\psi', q') = F' + A\nabla^2 q'. \tag{8}$$

We now assume that the perturbation is sufficiently small compared with the mean state that the $J(\psi', q')$ term in (8) can be dropped (this is discussed further in Section 4). Implicit in this is the assumption that the mean state is barotropically stable. Eq. (8) then becomes

$$\frac{1}{R}\frac{\partial q'}{\partial t} + J(\overline{\psi}, q') + J(\psi', \overline{q}) = F' + A\nabla^2 q'. \tag{9}$$

where $q' = R\nabla^2\psi'$ and $\psi = \nabla^2\psi' = 0$ along the boundary.

Eq. (9) describes the propagation of Rossby waves on the mean potential vorticity field $\overline{q}$, their advection by the mean flow $\overline{\psi}$, their generation by the wind stress curl perturbation F' and their dissipation by lateral mixing $A\nabla^2 q'$. The propagation is represented by the term $J(\psi', \overline{q})$. Since $\overline{q} = R\nabla^2\overline{\psi} + y$ the mean $\overline{q}$ contours are distorted from lines of latitude by the relative vorticity of the mean flow, the importance of which, for fixed E_L, is measured by the value of R. We shall compare the

effect of this distortion to that of advection by the mean flow represented by the $J(\overline{\psi}, q')$ term. The importance of this effect depends on the period of the wind forcing and, in particular, on the ratio of the period to the time taken for a fluid particle to advect the length of the western boundary current. It should be noted that when $\overline{\psi} = 0, \overline{q} = y$ and (9) reduces to the familiar equation

$$\frac{\partial}{\partial t}(\nabla^2\psi') + \psi'_x = F' + E_L\nabla^4\psi' \tag{10}$$

describing Rossby waves in a system linearized about a state of rest.

To solve (2) (and also (9)) we use a finite difference numerical method on a 50×50 grid. The Jacobian terms are finite differenced using the Arakawa method (see Mesinger and Arakawa, 1976). At each time step, a new value of $\nabla^2\psi$ ($\nabla^2\psi'$ in the case of (9)) is obtained. This is inverted to obtain the corresponding streamfunction ψ (or ψ') using the modified form of Gaussian elimination due to Lindzen and Kuo (1969).

Figure 1 shows the steady state solution obtained by integrating (2) with $R = 9.31 \times 10^{-3}$, $E_L = 1.35 \times 10^{-3}$ and steady wind forcing given by $\overline{F} = -\sin(y)$ ($y = 0$ is taken to be the southern boundary and the integration was started from a state of rest). This case uses the same value of R as Böning's experiment 5 but a value of E_L one and a half times larger (using the same value of E_L leads to a statistically steady state with a weak barotropic instability). We see that in addition to the usual Sverdrup interior flow feeding a western boundary current, a strong inertially recirculating subgyre is found in the northwest corner of the basin. As noted by Böning (1986), this feature is not unlike that found in eddy-resolving models (e.g. Holland *et al.*, 1983) and is associated with an increase in western boundary current transport, above the Sverdrup value, not unlike that observed in the Gulf Stream (e.g., Gill, 1971). It is also apparent that its presence significantly distorts the mean potential vorticity field $\overline{q}$ from the planetary vorticity y. It is this steady solution we adopt as our background mean state in this paper.

3. Model results

In this section, we describe results obtained by integrating (9) with

$$F' = \sin(\omega t)\sin y. \tag{11}$$

Three different values of ω are considered corresponding to nondimensional periods T of 132, 66 and 22. For a basin of size, the width of the North Atlantic, these are periods of 53, 26 and 9 days, respectively. For each case, the model is run until a steady, oscillating response is found. The background mean state $\overline{\psi}, \overline{q}$ is that shown in Figure 1, for which $R = 9.31 \times 10^{-3}$ and $E_L = 1.35 \times 10^{-3}$.

Figures 2–4 show the amplitude and phase of the computed streamfunction ψ' for the cases $T = 132$, 66 and 22, respectively. Three solutions are shown: (a) the full solution obtained by integrating (9); (b) the solution obtained by integrating (9) with the

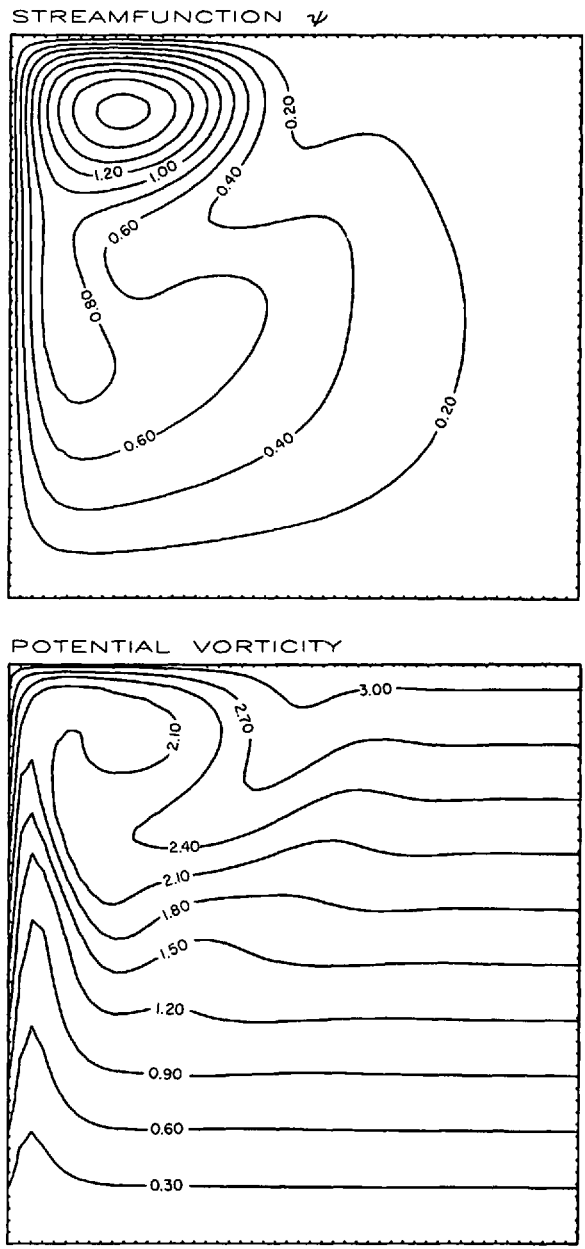

Figure 1. The steady solution obtained by integrating (2) from a state of rest with $R = 9.31 \times 10^{-3}$, $E_L = 1.35 \times 10^{-3}$ and steady wind forcing. Figure 1a shows the streamfunction $\bar{\psi}$ and Figure 1b the potential vorticity $\bar{q} = R\nabla^2\bar{\psi} + y$. The contour intervals are 0.2 and 0.3, respectively, with $\bar{\psi}$ in Figure 1a being normalized by the maximum Sverdrup transport associated with the wind forcing (this differs by a factor of π from the nondimensional system used in the text).

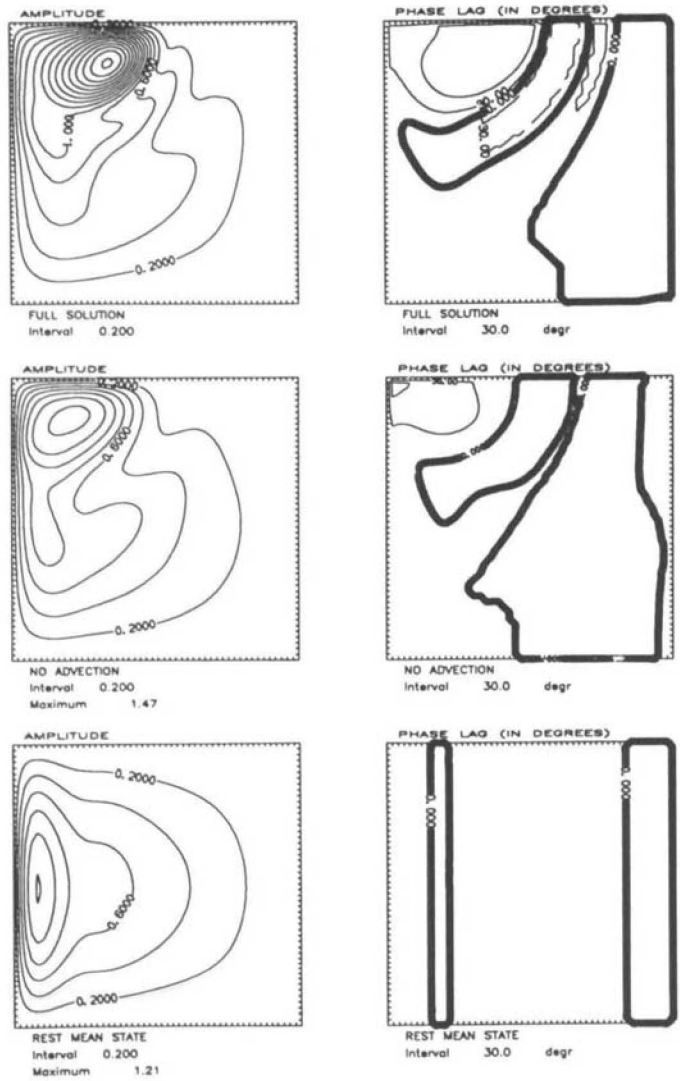

Figure 2. The amplitude and phase lag (compared to the wind) of the perturbation streamfunction ψ' due to oscillating wind forcing with nondimensional period 132. The amplitude is contoured at intervals of 0.2 and the phase at intervals of 30° over the range $-180°$ to $+180°$, dashed contours indicating negative phase. (Note that for the amplitude a value of 1 corresponds to the Sverdrup transport associated with the maximum wind stress curl perturbation.)

advection term $J(\overline{\psi}, q')$ dropped; and (c) the solution obtained by integrating (9) with $\overline{\psi} = 0$ and $\overline{q} = y$. The latter is the solution for the case when the background mean state is one of rest.

By comparing parts (a) and (b) of each figure with part (c), it is immediately apparent that the presence of a nonzero mean flow is quite effective at distorting the

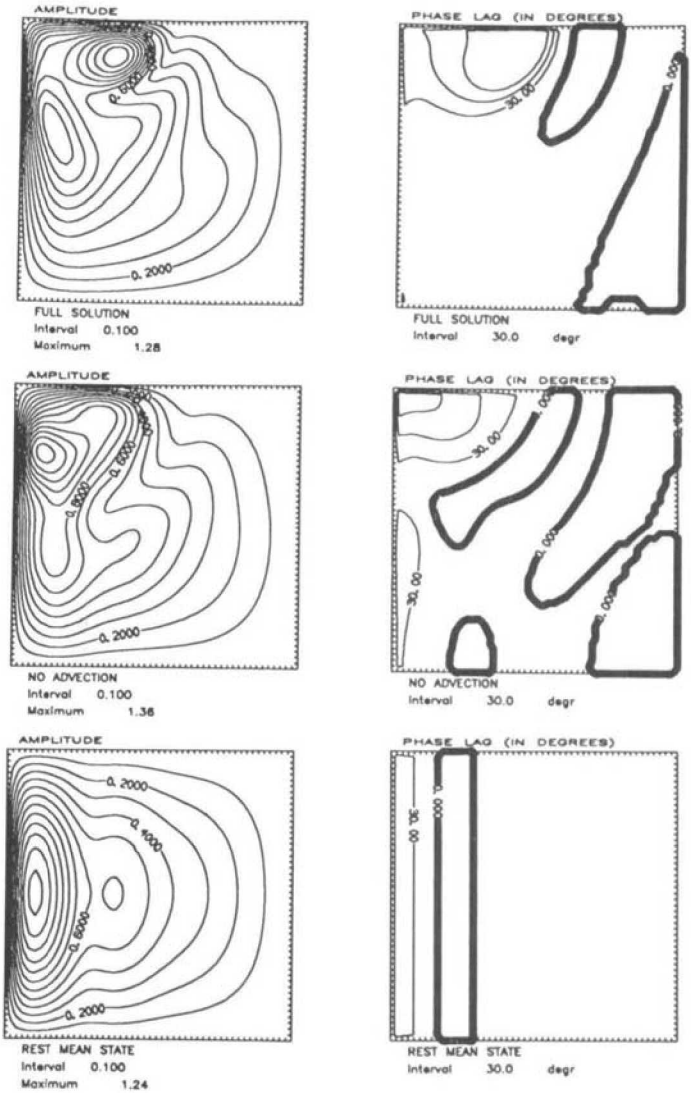

Figure 3. As in Figure 2 but for wind forcing with period 66. The amplitude is contoured with interval 0.1.

response, especially near the western boundary and in the inertial recirculation region. This is not surprising since it is precisely in these regions that the $\bar{q}$-contours are most distorted from lines of latitude and the velocities associated with the mean flow reach their greatest magnitude (see Fig. 1). Much of the structure we can see in part (a) of each figure is captured in part (b) and so can be attributed to the distortion of the $\bar{q}$-contours i.e. the $J(\psi', \bar{q})$ term in (9). However, advection also plays a role; in particular, in bending the phase lines within the inertial recirculation region and in

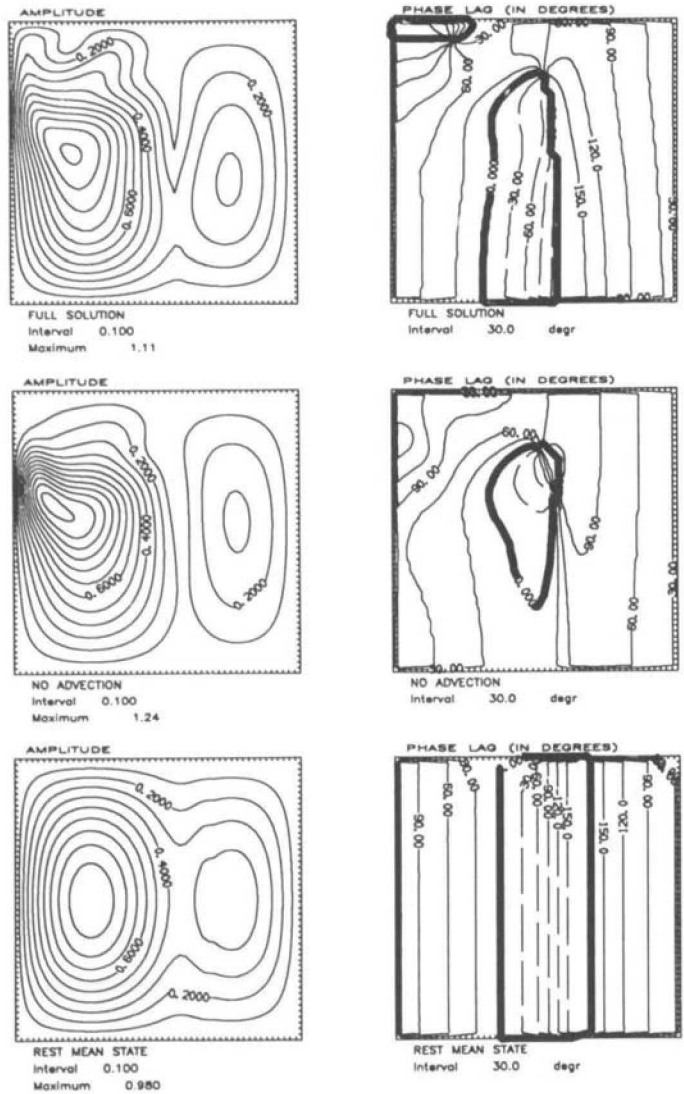

Figure 4. As in Figure 3 but for wind forcing with period 22.

shifting the region of maximum amplitude towards the eastern part of the recirculation region. This latter effect is more pronounced in the lower frequency, longer period cases (Figs. 2 and 3), but the tendency for it to occur can also be seen in Figure 4.

We now examine each case in greater detail. In the longest period case (Fig. 2), there is very little variation in phase across the basin when the mean state is one of rest (Fig. 2c). This indicates that the response at this period is a quasi-equilibrium one. In the presence of the nonzero mean state, some phase differences are introduced in association with the distortion of the $\overline{q}$-contours (Fig. 2b). In particular, a phase lag a

little over 60° is found in the northwest corner of the recirculation region and a tongue, in which the response slightly leads the wind, extends down from the northern boundary around the outer edge of the recirculation region. This is the region where, in Figure 1b, the $\overline{q}$ -contours are depressed southward as they are wound around the recirculation region by the mean flow. The effect of advection by the mean flow (Fig. 2a) is to bend the phase lines around the recirculation and to lengthen the phase lag. Interestingly, the transformation from the 30° contour in Figure 2b to the 60° contour in Figure 2a can roughly be accounted for by the advection time between their two positions. The region of slightly negative phase around the outer edge of the recirculation remains.

We have already noted that advection has the effect of shifting the region of maximum amplitude toward the northeast corner of the recirculation region, as can be seen by comparing Figure 2a with Figure 2b. This is further illustrated by Figure 5 in which we show the final steady state obtained by integrating (9) with a steady wind perturbation $F' = -\sin y$. In the case with the advection term $J(\overline{\psi}, q')$ dropped (not shown), the solution for ψ' is identical to that for the mean flow $\overline{\psi}$ shown in Figure 1a. This is not surprising since both satisfy the same equation i.e.

$$J(\psi', \overline{q}) = -\sin y + E_L \nabla^4 \psi' \tag{12}$$

where we have used $q' = \nabla^2 \psi'$. Introducing the advection term (Fig. 5) shifts the maximum to the northeast corner of the recirculation region, in a manner analogous to the shift we see between Figs. 2b and 2a, and leads to a substantial increase in amplitude. Of course, this experiment is rather artificial. Had we integrated (2) from a state of rest with the combined steady wind stress $\overline{F} + F'$, a different steady state would result from that obtained by simply adding $\overline{\psi}$ in Figure 1a to ψ' in Figure 5 (the problem, of course, is the neglect of the $J(\psi', q')$ term in (8)). Figure 5, nevertheless, illustrates the effect of the $J(\overline{\psi}, q')$ term on our steady, oscillating solutions when the time period of the oscillations is long compared to the adjustment time of the basin. Indeed, results (not shown) obtained for a nondimensional period T of 264 look quite similar to those shown in Figure 2, apart from some differences in phase. Similar results can be expected for nondimensional forcing periods corresponding more closely to the annual period.

Next we consider Figure 3. At this period ($T = 66$), we can see a slight phase lag near the western boundary in Figure 3c, indicating the presence of a weak, westward propagating Rossby wave. This wave is strongly frictionally attenuated as evidenced by its lack of penetration away from the boundary. The introduction of the nonzero mean state leads to a substantial increase in this lag. In association with the distortion of the $\overline{q}$-contours (Fig. 3b), a maximum lag a little over 100° occurs in the far northwest corner of the gyre. Introducing advection (Fig. 3a) further increases this lag with a maximum near 110° now being found in the northeastern part of the recirculation region. As we found before, advection bends the phase lines with the flow in the

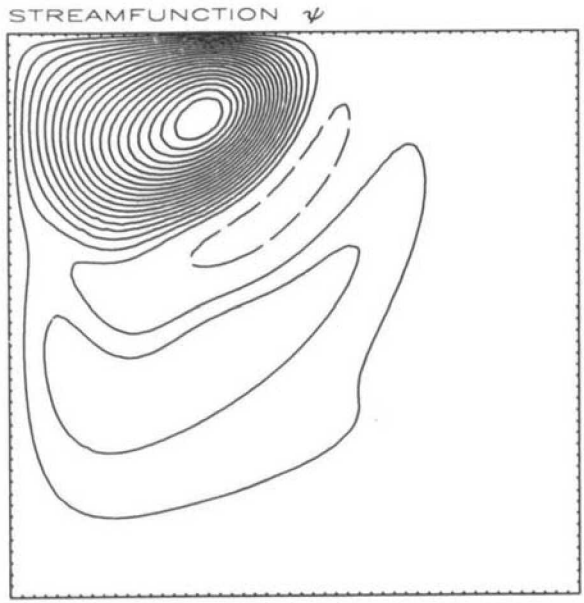

Figure 5. The steady solution obtained by integrating (9) from rest with a steady forcing perturbation F'. The contour interval is 0.3 and a value of 1 corresponds to the Sverdrup transport associated with the perturbation.

recirculation region and also shifts the region of maximum amplitude to the eastern part of the recirculation region. In this case, however, a secondary maximum remains near the western boundary. This indicates that at the shorter period we are considering here, compared with Figure 2, advection has less time to be effective, as we expect.

Figure 4 shows results in the shortest period case we have considered ($T = 22$). The rest mean state case (Fig. 4c) shows strong westward phase propagation with two peaks in amplitude; one in the western part of the basin and one in the east. It is easily shown that the minimum period for inviscid Rossby wave propagation in our basin is about 12.5. An interesting effect, once the nonrest mean state is introduced, is the suppression of westward propagation in the southern half of the basin in the case without advection (Fig. 4b). This is occurring despite the fact that the $\overline{q}$-contours are almost undisturbed from lines of latitude in this region. However, the distortion of the $\overline{q}$-contours is having the effect of restricting the north-south wavelength and by so doing, it is increasing the minimum period at which waves can propagate. The lack of propagation in Figure 4b suggests that the minimum period must be greater than 22 (if the maximum allowable north-south wavelength is reduced to one basin width, as seems reasonable, the minimum period is about 25). Interestingly, however, introducing advection (Fig. 4a) modifies the phase lines so that once again they are indicating westward propagation.

Overall, the effect of introducing a nonrest mean state is less dramatic in this case than in the two longer period cases. Nevertheless, longer phase lags are again

introduced in the northwestern part of the basin, the phase lines are clearly influenced by advection in the recirculation region (Fig. 4a) and there is a shift in the position of maximum amplitude. The distortion of the $\bar{q}$-contours shifts this maximum northwestward, toward the western boundary, whereas advection encourages a larger amplitude response within the recirculation region itself, although this effect is somewhat weaker than in the longer period cases.

We have also run our model with the wind stress curl forcing F' restricted to only certain parts of the basin. Figure 6 shows the model results when F' is set to zero in the northern half of the basin in the longest period case, $T = 132$. In the rest mean state case (Fig. 6c), the response is leaked northward by Rossby waves with southwestward phase propagation but a northward component to their group velocity (note the southwestward phase propagation in the northern half of the basin in Fig. 6c). The introduction of a nonzero mean flow distorts this phase propagation, especially in association with advection (Fig. 6a). Of particular interest, however, is the large increase in the amplitude of the response in the northern half of the basin. This occurs partly in response to the distortion of the $\bar{q}$-contours from lines of latitude (Fig. 6b), but is further enhanced by advection (Fig. 6a). These results suggest that wind stress variations to the south can lead to significant transport variations further north due to the presence of a mean flow. In the introduction, we noted that the seasonal variation of the surface wind stress curl over the western Caribbean is similar to that of transport through the Florida Straits. The above results suggest that the mean flow of the Loop Current/Florida Current system could play a role in communicating the effect of these wind stress variations northwards to the Straits. Clearly a more realistic model will be required to verify this.

4. Summary and discussion

We have discussed results from a flat-bottomed, barotropic ocean model driven by oscillating wind forcing. In particular, we have integrated the equations of motion linearized about a nonrest (barotropically stable) mean state corresponding to an ocean gyre circulation. The latter corresponds to one of Böning's (1986) solutions and was obtained by integrating the full nonlinear equations of motion with steady wind forcing until a steady state was reached. The resulting mean circulation has features corresponding to the vertically integrated flow field found in eddy-resolving general circulation models and has a Sverdrup interior, western boundary current and inertially recirculating subgyre in the northwest corner (for a subtropical gyre).

We have compared our solutions with those obtained when the mean state is one of rest and have shown that the presence of a nonrest mean state can significantly distort the response. These distortions can be related to two effects (i) the distortion of the mean potential vorticity ($\bar{q}$) contours from lines of latitude and (ii) advection by the mean flow. Both effects are most important near the western boundary and in the inertial recirculation region (it is in these regions that the $\bar{q}$-contours are most distorted

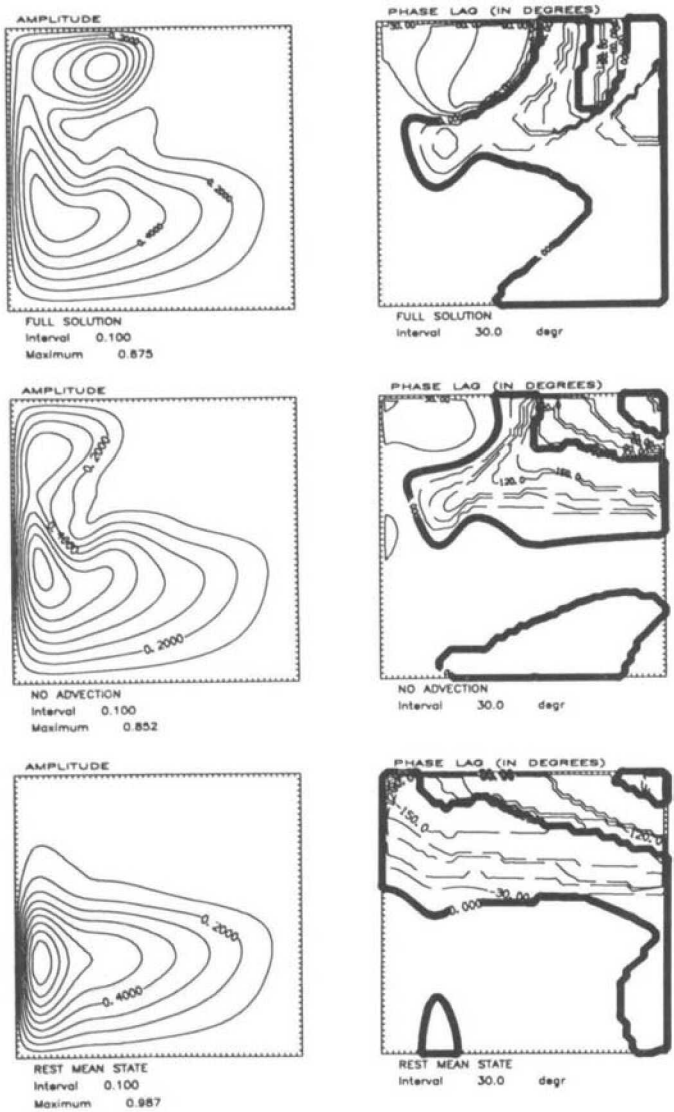

Figure 6. As in Figure 2 but with the wind stress curl forcing set to zero in the northern half of the basin. The period of the wind forcing is 132 in this case and the contour interval for the amplitude is 0.1.

and the currents associated with the mean flow are at their most intense). Significant phase lags and amplitude amplification are found in these regions compared with the solutions in the rest mean state cases.

The model described in this paper is obviously very simple. By using a flat-bottomed ocean model, we have excluded the important influence of bottom topography in

shaping the ambient potential vorticity field. Indeed, in the models of Anderson and Corry (1985b) and Greatbatch and Goulding (1989a, b), incorporating realistic bottom topography is crucial for obtaining the agreement they find between model results and data. On the other hand, using a flat-bottomed model enabled us to conveniently generate a realistic mean flow, following Böning (1986), avoiding the need to include the density stratification or to worry about the vertical structure of the mean flow and its possible interaction (and hence compatability) with the topography. Furthermore, despite the simplicity of the model, we expect many of the features exhibited by our solutions to also be found once bottom topography is included. The most robust are likely to be the phase lags associated with advection by the mean flow. However, the relative vorticity associated with the mean flow will distort the $\bar{q}$-contours in the same way they are distorted in our model from lines of latitude and this too will lead to modification of the response from the rest mean state cases.

We began in the introduction by noting that the linear barotropic model of Greatbatch and Goulding (1989a) could not properly account for the observed summer minimum in monthly mean sea level at Norfolk, Virginia (after corrections for atmospheric pressure variations and the seasonal heating cycle), despite its success at stations farther south. It was suggested that advection by the mean flow of the Gulf Stream, not included in their model, may offer an explanation of this. The results from the idealized calculations presented here support this view but also suggest that the distortion of the $\bar{q}$-contours due to the relative vorticity of the mean flow could be important. We have seen, in particular, how both these effects lead to downstream amplification of our model response compared to the rest mean state cases. Clearly, a repeat of Greatbatch and Goulding's calculations, including a representation of the mean flow, is required to properly verify the theory. Such a calculation would also throw light on the possible role of the mean flow in accounting for the observed amplitude of the seasonal variation in transport through the Florida Straits—a problem referred to in the introduction and at the end of Section 3.

To carry out a calculation like that referred to above will require a realistic representation for the mean circulation in the North Atlantic. Large eddy-resolving models, such as described by Holland and Bryan (1987), hold out the possibility of providing such a flow field in the near future. The possibility that the mean flow in the North Atlantic is barotropically unstable also means that such a calculation could indicate likely dominant modes of variability in the North Atlantic circulation, in the same way that barotropic instabilities of the climatological mean atmospheric circulation can be related to observed modes of atmospheric variability (Simmons *et al.*, 1983).

It was also suggested that advection by the mean flow of the Oyashio Current could provide an explanation for the time lag between the appearance of a positive wind stress curl anomaly in the North Pacific and the southward intrusion of the Oyashio along the coast of Japan noted by Sekine (1988a, b). We have seen that significant lags

related to both the advection time of the mean circulation and the distortion of the $\bar{q}$-contours are a feature of our model results. Whether these lags are sufficient to explain Sekine's observations will require detailed comparison with a more complex model than that considered here. Nevertheless, lags associated with the advection time for the circulation, and therefore of a month or so, are consistent with our results.

In this paper, we have considered only the equations of motion linearized about a mean state—we have not allowed feedback with the mean flow. However, at the seasonal time scale, wind stress fluctuations over the ocean are of a magnitude comparable to the annual mean (see, for example, Thompson and Hazen, 1983). It follows that in a flat-bottomed ocean model driven by observed wind forcing, the corresponding variations in transport are comparable to the annual mean, implying that the $J(\psi', q')$ term in Eq. (8) cannot be neglected in comparison with the $J(\bar{\psi}, q')$ term. Anderson and Corry (1985a) have pointed out, however, that bottom topography plays an important role at time scales of the annual period and less. In the North Atlantic, at least, this generally suppresses the amplitude of the barotropic response to wind, especially near the western boundary due to blocking of the signal by the shelf/slope topography. For example, in their studies of seasonal transport variability at the Florida Straits, the models of Anderson and Corry (1985b) and Greatbatch and Goulding (1989a) predict an annual cycle of amplitude 1-2 Sverdrups (the observed signal has amplitude nearer 4 Sv). This is much smaller than the 30 Sv annual mean transport through the Strait and is a direct consequence of the realistic bottom topography included in the models. It follows that if we were to repeat Greatbatch and Goulding's calculation, including a representation of the mean flow, linearized dynamics is more likely to be appropriate than in a flat-bottomed version of the same calculation, with the $J(\bar{\psi}, q')$ term often dominating $J(\psi', q')$. It therefore makes sense in the idealized calculations presented in this paper to consider the linearized equations of motion, even though we are considering a flat-bottomed ocean model, and to investigate the nonlinear feedback term $J(\psi', q')$ in a later calculation including both bottom topography and a mean flow.

Finally the connection between this work and that of Dewar (1989) should be pointed out. Dewar has extended the time-mean circulation theory of Rhines and Young (1982) to include time-dependent wind forcing. In his model, the barotropic response is assumed to be in a quasi-equilibrium, flat-bottomed Sverdrup balance with the wind stress curl forcing. It follows that, as in the earlier steady state theory, the $\bar{q}$-contours for the barotropic flow are lines of latitude which intersect the eastern boundary. This differs from our paper in which we have explicitly looked at effects arising from the distortion of these $\bar{q}$-contours from lines of latitude. His paper, however, is concerned with variability in the thermocline rather than with the barotropic transport variability we have looked at here. Future theories will, however, have to address both problems simultaneously—in effect a time-dependent circulation theory, including an inertial recirculation region.

Acknowledgments. This work has been funded by a grant from the Natural Sciences and Engineering Research Council of Canada. We are grateful to Allan Goulding and David Holland for their help with the model development. This is Ocean Science Centre contribution number 65.

REFERENCES

Anderson, D. L. T., K. Bryan, A. E. Gill and R. C. Pacanowski 1979. The transient response of the North Atlantic: Some model studies. J. Geophys. Res., *84* (C8), 4795–4815.

Anderson, D. L. T. and R. A. Corry. 1985a. Ocean response to low frequency wind forcing with application to the seasonal variation in the Florida Straits—Gulf Stream transport. Prog. in Oceanogr., *14*, 7–40.

—— 1985b. Seasonal transport variations in the Florida Straits: A model study. J. Phys. Oceanogr., *15*, 773–786.

Blaha, J. P. 1984. Fluctuations of monthly mean sea level as related to the intensity of the Gulf Stream from Key West to Norfolk. J. Geophys. Res., *89*, 8033–8042.

Böning, C. W. 1986. On the influence of frictional parameterization in wind-driven ocean circulation models. Dyn. Atmos. Oceans., *10*, 63–92.

Briggs, W. L. 1980. A new class of steady solutions of the barotropic vorticity equation. Dyn. Atmos. Oceans, *4*, 67–99.

Bryan, K. 1963. A numerical investigation of a non-linear model of a wind-driven ocean. J. Atmos. Sci., *20*, 594–606.

Dewar, W. K. 1989. A nonlinear, time-dependent thermocline theory. J. Mar. Res., *47*, 1–33.

Gill, A. E. 1971. Ocean models. Phil. Trans. R. Soc. Lond. Ser. A, *270*, 391–413.

Gill, A. E. and P. P. Niiler. 1973. The theory of the seasonal variability in the ocean. Deep-Sea Res., *20*, 141–177.

Greatbatch, R. J. and A. Goulding. 1989a. Seasonal variations in a linear barotropic model of the North Atlantic driven by the Hellerman and Rosenstein wind stress field. J. Phys. Oceanogr., *19*, 572–595.

—— 1989b. Seasonal variations in a linear barotropic model of the North Pacific driven by the Hellerman and Rosenstein wind stress field. J. Geophys. Res., *94*(C9), 12645-12665.

Holland, W. R. and F. O. Bryan. 1987. Progress in the WOCE Ocean Community Modelling Effort. EOS, *68* (44), (abstract), 1311.

Holland, W. R., D. E. Harrison and A. J. Semtner, Jr. 1983. Eddy-resolving numerical models of the large-scale ocean circulation, *in* Eddies in Marine Science, A. R. Robinson, ed., Springer-Verlag, Berlin, 379–403.

Huthnance, J. M. 1984. Slope currents and "JEBAR." J. Phys. Oceanogr., *14*, 795–810.

Lindzen, R. S. and H. L. Kuo. 1969. A reliable method for the integration of a large class of ordinary and partial differential equations. Mon. Wea. Rev., *97*, 732–734.

Maul, G. A., F. Chew, M. Bushnell and D. A. Meyer. 1985. Sea level variation as an indicator of Florida Current volume transport: Comparisons with direct measurements. Science, *227*, 304–307.

Mesinger, F. and A. Arakawa. 1976. Numerical methods used in atmospheric models. GARP Publication Series #17, World Meteorological Organization.

Munk, W. H. 1950. On the wind-driven ocean circulation. J. Meteorol., *7*, 79–93.

Rhines, P. B. and W. R. Young. 1982. A theory of the wind-driven circulation, 1. Mid-ocean gyres. J. Mar. Res., *40* (suppl.), 559–596.

Schott, F. and R. Zantopp. 1985. Florida Current: Seasonal and interannual variability. Science, *227*, 308–311.

Sekine, Y. 1988a. Anomalous southward intrusion of the Oyashio east of Japan 1. Influence of the seasonal and interannual variation in the wind stress over the North Pacific. J. Geophys. Res., *93* (C3), 2247–2255.

—— 1988b. A numerical experiment on the anomalous southward intrusion of the Oyashio east of Japan. Part I. Barotropic model. J. Oceanogr. Soc. Japan, *44* (2), 60–67.

Simmons, A. J., J. M. Wallace and G. W. Branstator. 1983. Barotropic wave propagation and instability, and atmospheric teleconnection patterns. J. Atmos. Sci., *40* 1363–1392.

Thompson, K. R. and M. G. Hazen, 1983. Interseasonal changes of wind stress and Ekman upwelling: North Atlantic, 1950–80. Tech. Rep. 1214, Can. Fish. and Aquat. Sci., Publ. Off., Dept. of Fish. and Oceans, Ottawa, Ontario, Canada, 13 pp.

Received: *4 May, 1989;* revised: *19 September, 1989.*